DOI: 10.1002/chem.201001776

Unexpected Deformations Induced by Surface Interaction and Chiral Self-Assembly of Co^{II}-Tetraphenylporphyrin (Co-TPP) Adsorbed on Cu(110): A Combined STM and Periodic DFT Study

Philip Donovan,[a] Abel Robin,[a] Matthew S. Dyer,[a] Mats Persson,*[a, b] and Rasmita Raval*[a]

Abstract: In a combined scanning tunnelling microscopy (STM) and periodic density functional theory (DFT) study, we present the first comprehensive picture of the energy costs and gains that drive the adsorption and chiral self-assembly of highly distorted Co^{II}-tetraphenylporphyrin (Co-TPP) conformers on the Cu(110) surface. Periodic, semi-local DFT calculations reveal a strong energetic preference for Co-TPP molecules to adsorb at the short-bridge site when organised within a domain. At this adsorption site, a substantial chemical interaction between the molecular core and the surface causes the porphyrin macrocycle to accommodate close to the surface and in a flat geometry, which induces considerable tilting distortions in the phenyl groups. Experimental STM images can be explained in terms of these conformational changes and adsorption-induced electronic effects. For the ordered structure we unambiguously show that the substantial energy gain from the molecule–surface interaction recuperates the high cost of the induced molecular and surface deformations as compared with gas phase molecules. Conversely, singly adsorbed molecules prefer a long-bridge adsorption site and adopt a non-planar, saddle-shape conformation. By using a van der Waals density functional correction scheme, we found that the intermolecular π–π interactions make the distorted conformer more stable than the saddle conformer within the organic assembly. These interactions drive supramolecular assembly and also generate chiral expression in the system, pinning individual molecules in a propeller-like conformation and directing their assembly along non-symmetric directions that lead to the coexistence of mirror-image chiral domains. Our observations reveal that a strong macrocycle–surface interaction can trigger and stabilise highly unexpected deformations of the molecular structure and thus substantially extend the range of chemistries possible within these systems.

Keywords: chirality · density functional calculations · porphyrinoids · scanning probe microscopy · self-assembly

Introduction

The controlled assembly of molecular building blocks on a well-defined substrate is one of the major keys in building molecular nano-devices.[1] The porphyrins are a class of molecules that are currently of great technological and scientific interest from this perspective,[1a,2] are prevalent in biological systems and perform, amongst numerous other roles, important oxygen-transport and light-harvesting functions.[2f,i,3] Porphyrins exhibit great flexibility and allow for a wide variation of functionalisation for specific electronic, magnetic and conformational properties that have given rise to promising technological applications in colorimetric gas sensors,[4] photonic wires, field-effect transistors (FETs), light emitting diodes (LEDs), catalysts, optical switches[5] and data storage.[6] An interesting development is the possibility of tech-

[a] P. Donovan, Dr. A. Robin, Dr. M. S. Dyer, Prof. M. Persson, Prof. R. Raval
Surface Science Research Centre and Department of Chemistry
University of Liverpool, Oxford Street
Liverpool, L69 3BX (UK)
Fax: (+44) 151 794 3896
E-mail: Raval@liv.ac.uk

[b] Prof. M. Persson
Department of Applied Physics
Chalmers University of Technology
Göteborg SE-412 96 (Sweden)
E-mail: mpersson@liv.ac.uk

Supporting information for this article is available on the WWW under http://dx.doi.org/10.1002/chem.201001776.

nologies based on porphyrin monolayers, which would require nanoscale control and detailed understanding of all relevant interactions involved in their adsorption and self-assembly.

Studies of ordered porphyrins and the related phthalocyanines on metal surfaces in solution[1b,2d,7] and ultra-high vacuum (UHV)[1a,2a,b,e–g,8] by using complementary surface science techniques, such as near-edge X-ray absorption fine structure (NEXAFS),[1a] X-ray photoelectron spectroscopy (XPS),[2b,f] and scanning tunnelling microscopy/spectroscopy (STM/STS)[1b,2g,8g,h,9] have provided insights into their geometric[1a,10] and electronic structure,[2f,9] conductivity, reactivity,[2f,11] catalytic properties[11] and chirality.[2a,8c,12] These studies[1a,2a,e,g] have also provided the first indications that the conformation of porphyrin molecules adsorbed both individually and in assemblies may involve molecular deformations that would be unfavourable in the gas phase,[2e,g] which suggests a strong influence of the molecule–surface interaction on the subsequent conformational adaptation. Despite these findings, it remains unclear which forces drive the observed strong molecular deformations and, therefore, a detailed understanding of the interactions that drive molecular adsorption, conformation and self-assembly of porphyrins at metal surfaces remains in its infancy.

Computational studies have been performed in the gas phase on the conformational flexibility of metallo-porphyrins,[2h,8g,h] porphyrin metalation[13] and porphine stacking through van der Waals interactions,[14] however, correctly describing the molecule–substrate interaction remains a major obstacle in understanding the adsorption of such complex molecules at surfaces. The importance of considering and understanding this interaction has been highlighted recently when combining it with intermolecular interactions to form supramolecular assemblies.[8h,15] It is, however, highly challenging to describe the molecule–substrate interaction in full for the type of assemblies under investigation. The most effective approach to address this issue is by computationally demanding periodic density functional theory (DFT) calculations, which allow useful insight into substrate contributions and the overall electronic and geometric properties of the assembled system. Periodic DFT calculations have been reported that detail the adsorption characteristics of Fe- and H_2-tetrapyridile porphyrins weakly adsorbed in a self-assembled layer[2a,16] and Pd- and Mn-porphines weakly adsorbed on the Au(111) surface.[17]

So far, porphyrin systems with strong molecule–surface interactions have not been studied in detail and remain poorly understood. Such systems are particularly attractive because of the possibility that surface contributions might compensate for the energetic cost of significant deformation away from vacuum conformations. This would enable the greater adaptability and versatility of porphyrin forms to be expressed and could open up unique surface-driven chemistries and new design opportunities. For strongly chemisorbed molecules with a substantial shorter molecule–surface distance, a semi-local functional provides the best available description of strong chemisorption and provides the best starting point for the understanding of the chemisorption bond and the possible deformations of the molecule.

Herein, we tackle this issue with a systematic study that combines STM and periodic semi-local DFT to investigate the conformational and electronic properties of Co^{II}-tetraphenylporphyrin (Co-TPP; Figure 1) on Cu(110). The Co-TPP/Cu(110) system allows for a strong macrocycle–surface interaction with a short bonding distance, has potentially interesting electronic and magnetic features and is sufficiently simple for the application of periodic DFT modelling because it possesses no reactive substituent groups that could strongly influence the porphyrin assembly.[2d] Semi-local DFT has been shown to be inadequate in its description of long-range dispersion interactions. Therefore, to account for the π–π interactions between the phenyl groups of neighbouring molecules we used an efficient implementation[18] of a post-correction scheme[19] of the Langreth–Lundqvist van der Waals density functional (vdW-DF).[19–20] By treating the molecule–metal interaction with the semi-local functional, we will underestimate any dispersion interaction between the molecule and the surface. However, because there is no well-established method for the inclusion of dispersion interactions for strongly chemisorbed molecules on metal surfaces and the chemisorption interaction is expected to dominate, we feel at this stage that semi-local DFT provides the best approach for capturing the chemisorption interaction.

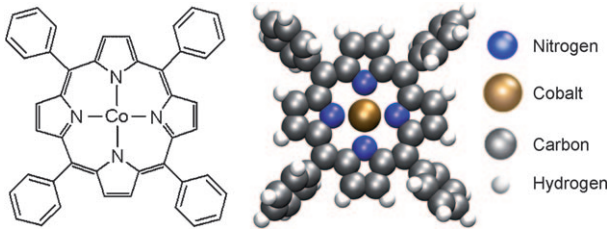

Figure 1. Chemical and structural representations of Co-TPP.

A comprehensive picture of the full molecule–surface system is presented, allowing for a quantitative description of costs and gains of the relevant interactions, including the strong molecule–metal interactions that drive the substantial porphyrin deformation and intermolecular π–π interactions that also contribute to the subsequent chiral self-assembly. Furthermore, a conformational and energetic comparison with the adsorption of isolated single molecules is performed.

Results and Discussion

Self-organised Co-TPP structures on Cu(110)

Experimental STM and low-energy electron diffraction (LEED) results: STM data taken at room temperature reveal that several distinct organised structures can be created by the adsorption of Co-TPP on Cu(110), depending on

both coverage and dosing flux. Herein, we concentrate on the most prominent superstructure, which occurs over a large coverage regime and is formed at room temperature under low flux conditions, referred to as structure A. Large-area STM data from this structure are presented in Figure 2 and show the co-existence of two mirror domains, the growth directions of which diverge from the [001] axis by $\pm(20\pm2)°$ respectively. The system, therefore, possesses chiral domains, denoted λ and δ. Following deposition at room temperature, these organised domains are observed to nucleate and grow with time, and are capable of reaching dimensions of 1 μm^2.

Figure 2b–e displays detailed, small area STM images obtained from each chiral domain. These reveal a highly organised domain structure. From the regular patterns observed, we can identify the repeat unit mesh directly from calibrated STM images, as shown in green in Figure 2f and g. Both chiral domains possess structures that are commensurate with the substrate and are described by using standard convention[21] as tensors:

$$A^{\lambda} = \begin{bmatrix} 2 & 4 \\ -6 & -2 \end{bmatrix}$$

$$A^{\delta} = \begin{bmatrix} -6 & 2 \\ 2 & -4 \end{bmatrix}$$

LEED data from this overlayer (Figure 3) are also consistent with this repeat unit, with coexisting mirror unit meshes observed. Each unit mesh accommodates a single Co-TPP molecule, and each molecular position is, therefore, associated with a number of bright spots and a dark area in the STM image. By positioning the Co-TPP molecules onto the STM images such that each bright spot corresponds to one phenyl group, we obtain a highly ordered and close packed layer in which the molecules appear with reasonable dimensions when compared with the gas-phase conformation (Figure 2f, g). In this configuration, we see that the STM images show little or no contribution from the Co-TPP core, although some negative bias images show a weak spot at the cobalt position. Using the centres of the bright spots associated with individual phenyl rings to determine distances x and y, as shown in the inset in Figure 2g, we calculate the molecular aspect ratio (x/y) in structure A to be 1.1.

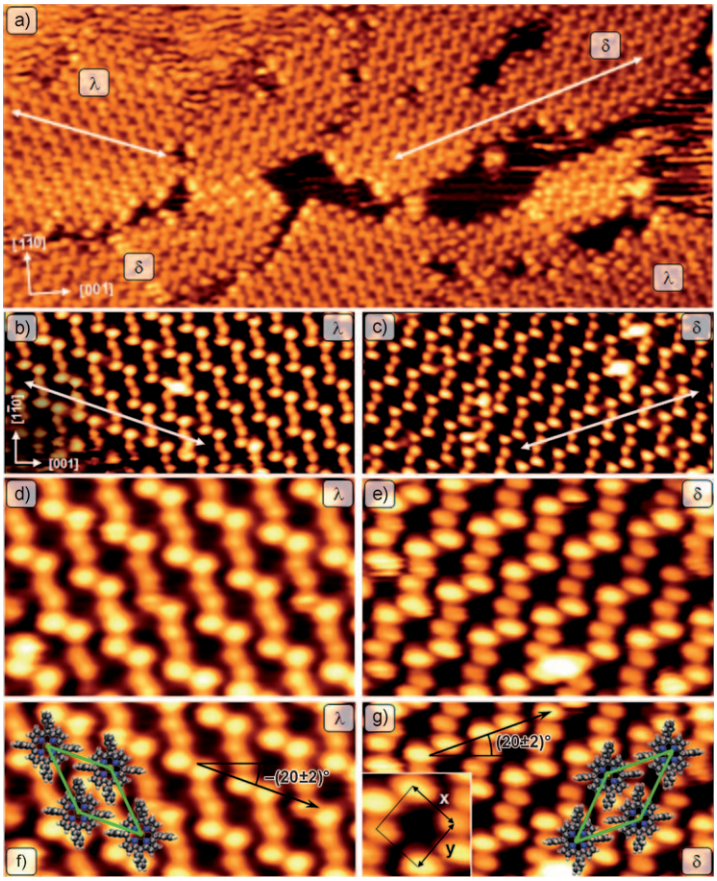

Figure 2. Co-TPP assembly on Cu(110) showing the λ and δ chiral domains of structure A. Bright spots represent significant contributions from the phenyl rings (see the main text) whereas the porphyrin cores image as dark areas. Arrows represent the main growth directions of both chiral domains. a) Large area (542×242 $Å^2$) image showing coexisting chiral domains, I_T=0.48 nA, V=1250 mV. Detailed images of the two chiral domains are shown in b) 140×65 $Å^2$, I_T=0.32 nA, V=670.5 mV; c) 140×65 $Å^2$, I_T=0.49 nA, V=670.5 mV; d) 80×50 $Å^2$, I_T=0.38 nA, V=734.8 mV; e) 80×50 $Å^2$, I_T=0.21 nA, V=611.3 mV; the copper axes in b) apply to all subsequent images. f), g) Molecules overlaid on sections of d) and e), respectively, showing the unit meshes. Chiral directions are shown relative to the Cu [001] axis. Inset: The aspect ratio of adsorbed Co-TPP.

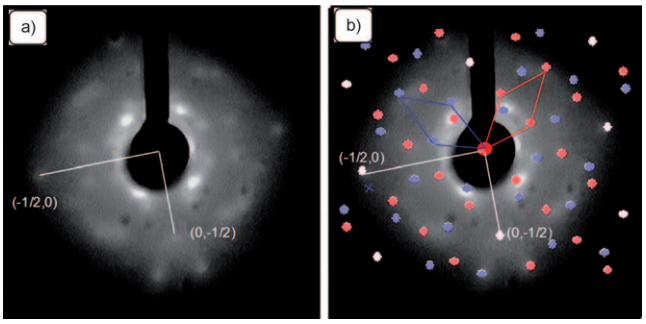

Figure 3. LEED pattern generated by structure A on Cu(110). a) LEED image taken at 20 eV. b) Comparison with simulated LEED pattern[22] including both chiral domains of structure A represented by small blue and red circles. Spots identified with both domains are shown in white. Note that the adlayer is highly sensitive to electron beam damage, making it difficult to capture LEED images.

Adsorption site, molecular deformations and STM simulations: To derive the specific adsorption site for Co-TPP in structure A and to obtain further insight into the bonding and conformation of the adsorbed Co-TPP molecule, we used the unit mesh of the λ domain to perform periodic DFT calculations of the full system, with particular focus on the molecule–metal and molecule–molecule interactions that drive the observed chiral self-assembly.

DFT calculations by using periodic boundary conditions were carried out to find the energetically preferred adsorption site for the Co-TPP molecules within structure A. We found a strong preference for molecular adsorption with the central cobalt atom at the short-bridge site (see Figure 4), with adsorption at the top, hollow and long-bridge sites calculated to be less stable by +29, +70 and +112 kJ mol^{-1}, respectively.

Our calculations show large molecular deformations away from the preferred conformation in vacuum when Co-TPP adsorbs at the short-bridge site (Figure 4). Porphyrin deformations can occur both within the macrocycle and in the attached side functional groups. The DFT calculations of Wölfle et al.[2h] give a useful insight into the energy cost of various distortions in the gas phase for selected metal–TPP molecules. Considering the macrocycle first, our calculations reveal that the adsorbed molecule shows only minor deformation from planarity, with the macrocycle curved but not saddled (see Figure 4). Cobalt porphyrins have been shown to possess enhanced resistance to distortions of the macrocycle, even in the gas phase.[2h] We show below that this planarity is additionally favoured by the nature of the interaction between the macrocycle and the copper surface. Interestingly, we found that the cobalt atom in the core is held just 2.2 Å above the surface plane, which corresponds to a shortest Co–Cu length of 2.5 Å (shown in Figure 4) and significant deformations in the phenyl groups are consequently observed. This contrasts with the observations made by Zotti et al.,[16] in which a weak molecule–substrate interaction between H_2-tetrapyridylporphyrin (TPyP) and an Ag(111) surface results in a large molecule–surface separation of 5.6 Å and mainly preserves the original conformation of the molecules.

Turning to the deformation of the phenyl groups, we follow Wölfle et al.[2h] in defining the tilt angle, Φ, as the angle between the plane of the macrocycle and the σ bond connecting phenyl rings to the core. Twist (dihedral) angles, Θ, describe the rotations of the phenyl rings around the same σ bond and are defined as the angle between the phenyl ring plane and the surface plane (Figure 4). In the lowest energy configuration calculated for the isolated molecule in the vacuum, one finds that tilting distortions are energetically costly and the gas-phase system displays only a small distortion of $\Phi = 176°$. In contrast, twist distortions are less costly and a large range of angles between 90 and 60° can be tolerated in the gas phase.[2h] As a result, significant dihedral twists are commonly observed when adsorbing porphyrin derivatives on metal substrates and may experimentally be accessible by determining the molecule's aspect ratio from STM data.[2e,8f] The deformations we observe for Co-TPP assembled on Cu(110) in structure A are the result of a compromise between two interactions: an attractive interaction between the Co-TPP core and the surface and a repulsive interaction between the phenyl rings and the surface. When adsorbed at the short-bridge site, the phenyl groups align with and accommodate themselves in the corrugations of the Cu[001] and Cu[1$\bar{1}$0] rows by a combination of tilting and twisting. Due to the intrinsic anisotropy in the system endowed by the substrate, two pairs of diametrically opposite phenyls exist that are clearly identified by their different twist angles (see Figure 4). Our calculations show that the first pair of phenyls, aligned with the [001] rows, shows Θ angles of 78 and 88° which lie within the range of values that can be expressed in the gas phase conformation. However, the proximity of the surface causes substantial and costly Φ angles of 144 and 145° in this pair, which is a large deviation from the vacuum configuration. The interaction between the second phenyl pair and the substrate is significantly different. Here, the adsorption site dictates that the phenyl centres align on top of the close-packed [1$\bar{1}$0] rows. The calculated Θ angles of 60 and 63° are close to those adopted in the vacuum,[2h] and are sufficient to move the hydrogen atoms away from the copper atoms (Figure 4). Slightly less costly Φ angles of 154 and 152° are required in this pair to allow accommodation close to the surface.

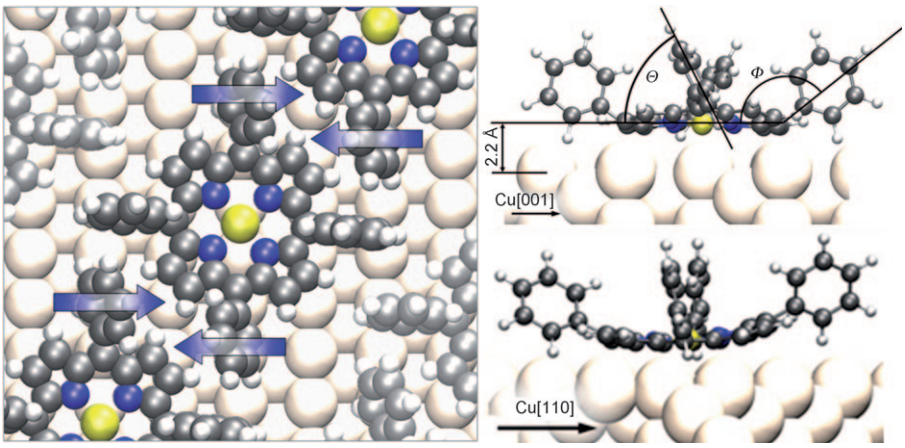

Figure 4. Molecular conformation of Co-TPP within structure A. Left: Adsorption site of the minimum energy conformation calculated by DFT. The twisting of the phenyls relative to the core (arrows) gives the molecule a chiral propeller-like conformation. Top right: Side view along the Cu [1$\bar{1}$0] axis of Co-TPP; the tilt (Φ) and twist (Θ) angles are altered significantly with only minimal deformation of the core. Bottom right: Side view of Co-TPP viewed along the Cu [001] axis.

The Co-TPP/Cu(110) structure shown in Figure 5 provides a good basis for understanding the features observed in experimental STM data. Firstly, due to the large phenyl tilt angles of the adsorbed Co-TPP, we can attribute the lack of discernible core structure in the STM images to a largely topographical origin; a result of the greater height of the phenyl groups relative to the core. We also observed a good agreement between experimental and calcu-

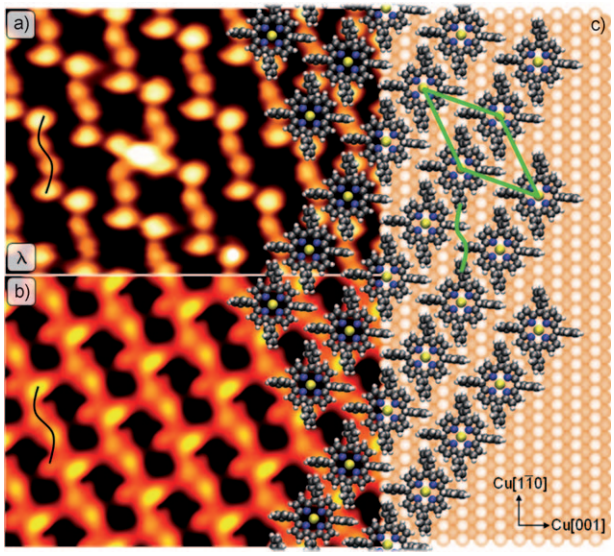

Figure 5. A good agreement is observed between experimental and simulated STM images for structure A. a) STM image of the λ domain, recorded at $V=449.8$ mV, $I=0.32$ nA. b) The corresponding STM image of the structure calculated at $V=450$ mV. The contour range for b) is 9.7–10.95 Å. c) The molecular overlayer of a real-space model of the self-assembled λ domain of Co-TPP/Cu(110) shows good overlap with both a) and b). The unit cell and the S-like structure are shown in green.

lated STM data for the short-bridge adsorption site within the

$$\begin{bmatrix} 2 & 4 \\ -6 & -2 \end{bmatrix}$$

assembly of the λ domain (Figure 5). Both the stretched S-like structure consisting of phenyl groups from four neighbouring porphyrins and the characteristic dark porphyrin cores are reproduced well by the calculated STM images (Figure 5). The calculated aspect ratio of 1.1, by using the topmost hydrogen atoms from each phenyl ring, agrees with the value derived from STM images. It can be seen from Figure 4 that the deviation from square is a result of the different twist angles of the two pairs of phenyl rings and not from macrocycle distortions.

The lowest energy conformation, as shown in Figure 4, is asymmetric: the cobalt atom is slightly offset from the short-bridge site and all four phenyl groups are oriented differently. This gives rise to the asymmetry seen in the calculated STM image in Figure 5 in which the topmost feature of the S-like structure is brighter than the bottom. Due to the large number of degrees of freedom with such a large molecule, there are many similar conformations with very similar energies that correspond to nearby local minima on the potential energy surface and an exhaustive search for the global minimum within these is not feasible. Several symmetric adsorption conformations were also found with the cobalt atom above the short-bridge site, which lead to more symmetric STM images, but these were slightly less stable by 3 kJ mol^{-1}. Nevertheless, all the low-energy conformations of Co-TPP adsorbed at the short-bridge site had qualitatively the same adsorption geometry, both in terms of the deformation of the macrocycle and the orientation of the phenyl substituents, and our conclusions would not be affected by choosing any of these structures. In fact we may conclude from this analysis that several conformations with very similar geometries and energies exist simultaneously at room temperature. Data from two alternative stable conformations with the cobalt atom situated above the short-bridge site are shown in the Supporting Information for comparison.

In addition to the deformation of the molecule away from its preferred conformation in vacuum, the positions of the atoms in the underlying copper substrate are also seen to change upon adsorption (Figure 6). The largest substrate deformation is observed beneath the porphyrin macrocycle. Eight of the ten top-layer copper atoms directly below the carbon atoms in the macrocycle are drawn out of the surface and towards the carbon atoms by up to 0.1 Å (red). The closer of the two top-layer copper atoms to the central cobalt atom and six of the second-layer copper atoms (green) below the centre of the macrocycle move down into the surface by a similar distance. The four top-layer copper atoms below the phenyl rings also move down into the surface by 0.1 Å and show some additional lateral displacements. The remaining two top-layer copper atoms in the unit cell have only negligible displacements away from their clean surface positions. We note that the asymmetry in the

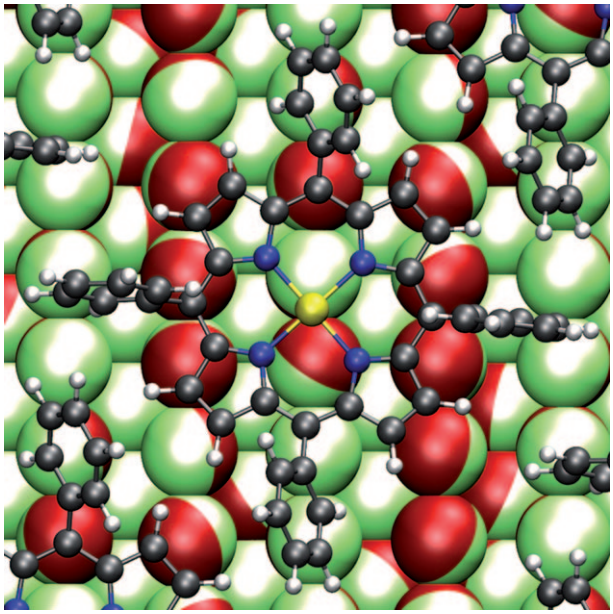

Figure 6. The directional displacement of copper atoms following adsorption of Co-TPP within structure A. The positions of copper atoms in the relaxed bare copper surface are represented in green, and those of the copper atoms with the Co-TPP molecule present are overlaid in red. Copper atoms appear red if they have moved out of the surface. Copper atoms that appear part green and part red represent a lateral motion away from the green position and towards the red.

overall Cu displacement pattern reflects the small asymmetry in the adsorption geometry of the molecule which in turn is echoed in the STM image, as described in the previous paragraph.

The calculated energy cost to deform the molecule from its optimised vacuum conformation[2h] to its adsorbed conformation within the self-assembled adlayer on Cu(110) is 206 kJ mol^{-1}. In addition, a concomitant deformation of the copper surface occurs at a cost of 31 kJ mol^{-1}, which means that the total cost of deformation of the molecule and substrate is $E_{COST}=237$ kJ mol^{-1}. The necessity of including a deformable substrate in theoretical approaches to energetic analyses of adsorbed porphyrins is clearly highlighted by the significant difference the addition of the surface reconstruction makes to the total cost. Importantly, there must be a substantial energy gain from the molecule–surface interaction to offset this large deformational energy cost, as discussed below.

The molecule–surface interaction: We examined the nature of the molecule–substrate interaction by calculating the difference in electron density between the full adsorbate–surface system and the isolated systems. The spatial effect of adsorption on the electron density can be seen in the plot of electron density difference (Figure 7a). The calculation shows an increase in electron density between the uppermost rows of copper atoms and both the cobalt atom and the macrocycle. This localisation of electron density between the molecules and surface stabilises the system, as in the case of a conventional covalent bond, and is also responsible for maintaining the planarity of the macrocycle. It should be noted that the nitrogen atoms of the macrocycle pyrroles play no part in the adsorption.

In an attempt to understand the molecule–substrate interaction in more detail, the density of states for the adsorbed molecule and surface were projected onto the molecular orbitals (MOs) of the molecule in vacuum with the same geometry and arrangement as on the surface. The resulting molecular orbital projected density of states (MO-PDOS) is presented in Figure 7b. The MO labelled d_{z^2} is predominantly formed from the Co d_{z^2} orbital and is only singly occupied in vacuum. Upon adsorption it is clear from Figure 7b that the d_{z^2} MO is broadened and becomes fully occupied. This eliminates the enhanced tunnelling pathway observed in STM studies of similar systems[1b,2b,9] and contributes to the lack of core structure in the STM data. In addition, the width of the d_{z^2} peak reflects substantial interaction with the metal surface. Electron transfer into the previously unoccupied LUMO and LUMO+1 orbitals is also seen; these orbitals are almost degenerate in the gas phase and are predominantly of π character. The peaks from these orbitals are also broad and the orbitals become roughly half-filled. The states that become occupied have energies in the bottom half of the MO-PDOS peaks and are expected to have mainly bonding character between the molecule and the surface. As an example of the effect of adsorption on the previously occupied MOs based on the macrocycle of Co-TPP, we show the MO-PDOS for the two highest occupied π MOs (1π and 2π) of the isolated molecule. Both of these orbitals are split into different broad peaks and show a strong interaction with the surface, but because they remain fully occupied they are not involved in the charge transfer between molecule and substrate and, therefore, do not contribute to the chemisorption interaction. Overall, the transfer of electrons into the d_{z^2}, LUMO and LUMO+1 orbitals is in agreement with the spatial distribution of electron density difference seen in Figure 7a. The overall extent of the electron transfer from the surface to the molecule was calculated as 1.3 e$^-$ by using the Bader scheme[23] to partition the electron density between the molecule and the surface.

The electron transfer and the interaction of the MOs with the metal surface, as shown in Figure 7, give rise to strong chemisorption with both ionic and covalent character. These bonding interactions with the d_{z^2} and LUMO and LUMO+1 orbitals are the source of a large attractive interaction energy $E_{MOL-SUR}=-335$ kJ mol^{-1}, calculated by taking the isolated molecule and bare surface in the same deformed configurations as when the molecule is adsorbed as a reference. The large magnitude of $E_{MOL-SUR}$ more than recuperates the considerable energy cost ($E_{COST}=+237$ kJ mol^{-1}) calculated for the conformational deformations.

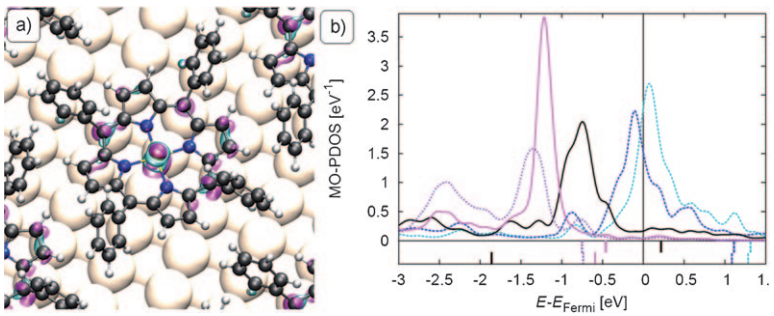

Figure 7. a) The difference in electron density between the adsorbed molecule and the isolated molecular and substrate systems. The pink (light blue) areas show the increase (decrease) in electron density. b) The density of states of the adsorbed molecule projected onto orbitals in the isolated molecular system; LUMO+1: ----, LUMO: ----, d_{z^2}: ——, 2π: ——, 1π: •••••. The sum of the majority and minority spin contributions are shown. The energies for the orbitals in the isolated system are shown as bars at the bottom of the plot with energy levels for the majority spin shown below those of the minority spin. The energy zero for the isolated energy levels is taken as the midpoint between the HOMO and the unoccupied Co d_{z^2} spin-orbital such that orbitals that are occupied (unoccupied) in the isolated system are shown as negative (positive) energies.

Inter-molecular interaction: Here we define the attractive inter-molecular interaction energy in the structure A domain as the energy difference between a single isolated molecule and a single molecule in the isolated molecular layer.

The configurations of the molecules are all taken to be identical to the molecule in the adsorbed layer. This interaction will have a large component from the π–π interactions between the phenyl groups, which are poorly described by DFT using standard functionals. However, the vdW-DF gives a good account of the π–π interaction as demonstrated by calculations of various benzene dimer configurations similar to those present in our system.[24] By using the vdW-DF post-correction scheme, we find that the attractive interaction energy, $E_{M-M} = -58\ kJ\,mol^{-1}$, is substantially larger than the value of $-7\ kJ\,mol^{-1}$ obtained by using PW91. As discussed below, this energy gain from intermolecular interactions is assumed to be responsible for preferential domain formation at room temperature.

Attractive interactions between phenyl groups in structure A occur in different configurations, and are classified as T, parallel displaced (PD)[25] and combinative PD/T interactions, as shown in Figure 8b for the δ domain. They are maximised by involving each phenyl ring in two of the three interacting configurations, thus forming staggered rows of high interaction that can be symbolised by the S-like structure indicated in Figures 5 and 6. We define the phenyl ring centroid as the centre of mass of the carbon ring. Calculated at 4.9 Å, the inter-centroid separation for the T configuration of phenyls in structure A (red lines in Figure 8b) is identical to the minimum energy separation for benzene dimers.[25] The inter-centroid separation for the PD configuration (green lines in Figure 8) of 5.2 Å is greater than the value of 3.75 Å quoted for the optimised configuration.[25a,c] All other phenyl–phenyl configurations have a significantly larger inter-centroid distance and their interactions are almost negligible.

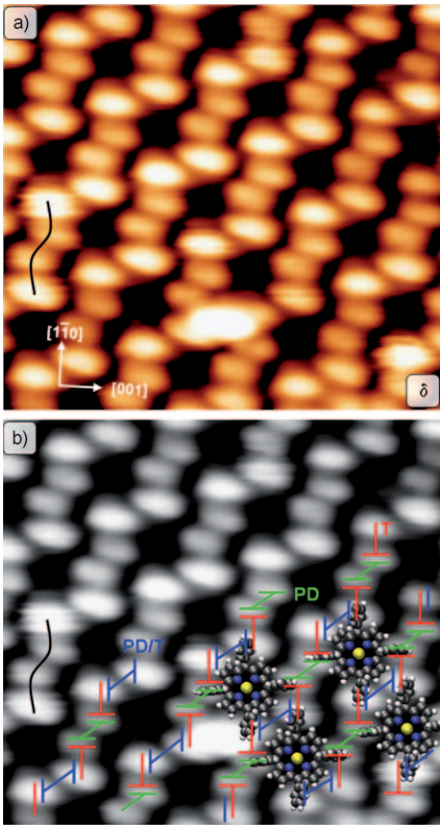

Figure 8. Inter-molecular interactions in the δ domain of structure A. PD (green lines), T (red lines) and PD/T (blue lines) phenyl–phenyl interactions form lines of high interaction that correspond to the indicated S-like structure (cf. Figure 4). Image conditions: $58 \times 56\ Å^2$, $V = 650$ mV, $I = 0.52$ nA.

Net energy balance: By substituting the interaction energies derived in the previous sections into Equation (1), we can calculate the net interaction energy E_{NET} (or the negative adsorption energy). This is defined as the difference in energy between the adsorbed system and the fully relaxed isolated molecule and bare substrate.

$$E_{NET} = E_{MOL-SUR} + E_{M-M} + E_{COST} \quad (1)$$

By using the energies from our calculations, the net interaction energy for structure A is calculated as follows: $E_{NET} = -335\ kJ\,mol^{-1} - 58\ kJ\,mol^{-1} + 237\ kJ\,mol^{-1} = -156\ kJ\,mol^{-1}$.

Disregarding the contribution from inter-molecular interactions, the substantial gain from the macrocycle's interaction with the copper substrate alone more than recuperates the total cost of both molecule and substrate deformations. In fact, this gain is so considerable that even greater molecular deformations would be accessible and we assume that strong molecule–substrate interactions have the potential to unlock severe conformational distortions and thus different and unexpected chemistries for other porphyrin/surface systems.

Chirogenesis: Chirogenesis, the induction of chirality in intrinsically achiral components, is evident at both the molecular and the supramolecular level from the LEED and STM images of organised Co-TPP structures on Cu(110). The distinct pattern of phenyl–phenyl interactions around individual molecules in the organised structure (see Figure 9) explains the induction of supramolecular chirality; the directionality of these interactions, indicated by the green (PD) and blue (PD/T) ovals in Figure 9, determine whether the domain orients at $+(20 \pm 2)°$ or $-(20 \pm 2)°$ with respect to the Cu[001] axis, thus the repeat mesh of the organisation breaks both mirror-symmetry planes of the underlying Cu(110) surface.

Furthermore, it can be seen from the DFT-calculated molecular conformation in structure A (Figure 4) that the twisting deformations of the phenyls break the local mirror symmetry of the system. The twist is small for the pair of phenyls aligned along the [001] rows, but the substantial and matching (anti)clockwise twists of the second phenyl pair endow each adsorbed molecule with a distinctive propeller-like conformation and lead to a strong expression of chirality at the individual molecule level. Prior to 2D assembly, the phenyls aligned with the [1$\bar{1}$0] axis are presumably free to choose between energetically equivalent twists of about

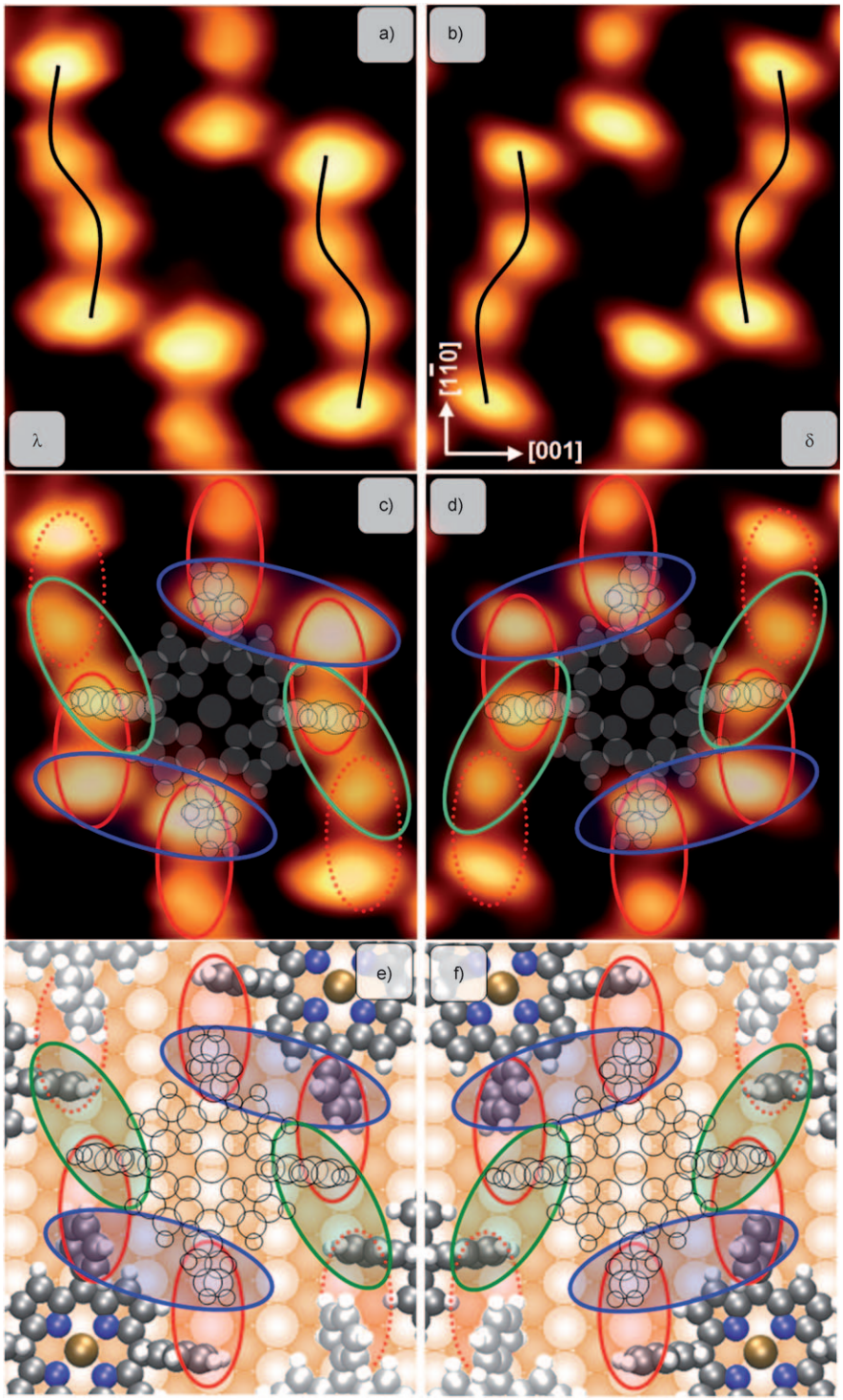

Figure 9. Expression of chirality in structure A. Enlarged sections of STM images from Figure 2b and c show individual molecules from the a) λ and b) δ domains. Lines of high interaction are indicated and the copper axis in b) applies to all figures. c), d) Overlay of the PD interactions as green ovals, PD/T interactions as blue ovals and T-type interactions as red ovals for single molecules in both domains. Dotted red ovals are T-type interactions that are not associated with the central molecule. The same interactions are shown on the real-space structures in e) and f).

±65° to accommodate the substrate corrugations. However, upon the formation and optimisation of all PD, PD/T and T interactions, the phenyl pairs are forced to twist in the same sense, that is, clockwise or anticlockwise, to minimise the repulsive forces between the molecules. This pins each molecule into the well-defined propeller-like conformation shown in Figure 4 and results in the induction of molecular, or local, chirality.

Co-TPP single-molecule adsorption and conformation

The molecular conformation of Co-TPP discussed for structure A differs remarkably from that observed for the same or closely related molecules adsorbed on Ag(111) or Cu(111), for which a saddle-shaped conformation has generally been determined by using STM and NEXAFS.[1a,2e,h,i,26] Weber-Bargioni et al. reported that a saddle-shaped molecular conformation is also found within the small domains formed when Co-TPP is adsorbed on Cu(111).[2g] This poses a question: what drives the unexpected adsorption geometry of Co-TPP on Cu(110) with strong phenyl tilt distortions within structure A domains? Firstly, the open (110) surface of a fcc metal is generally more reactive than the close-packed (111) face and therefore, the molecule–substrate interaction is probably weaker on Cu(111) than on Cu(110); secondly, from the discussion of structure A we conclude that the substrate corrugation plays an important role in molecule orientation and results in the phenyl groups aligning along the major Cu(110) axes. It is now interesting to investigate whether this observation holds for single isolated molecules adsorbed on Cu(110) as well.

Single Co-TPP molecules proved difficult to image under the conditions of this experiment. However, scattered single molecules showing no significant interaction with other molecules are frequently observed near organised domains of

Co-TPP molecules. They preferentially occupy step sites and confined areas, but are also found on terraces. Figure 10 shows a few single molecules surrounding part of a structure A domain, but not associated with the assembly. Interestingly, it can be seen that the molecules forming the outermost row of the organised structure are unaffected by their single free phenyl and show the same structure as those within the domain.

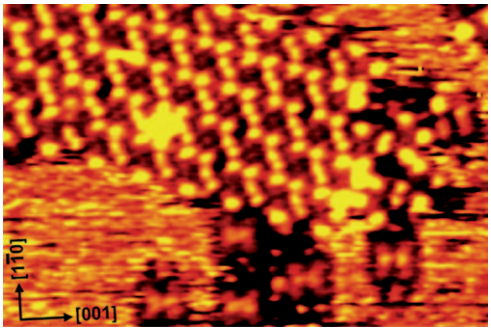

Figure 10. STM image showing part of a structure A island and a domain border. Isolated Co-TPP molecules can be seen below the ordered structure, appearing distinctively different. Image conditions: 105×155 Å^2, $I=$ 0.4 nA, $V=1250$ mV.

However, isolated molecules not attached to a domain are clearly imaged in a distinctively different way to those within the domains, namely, the core becomes more prominent and the phenyl groups image weaker. Furthermore, the single molecules and substrate share common mirror symmetry planes. These features have been shown to indicate core deformations that lead to a saddle-shaped molecule.[6]

Having established a short-bridge adsorption site for molecules in structure A, we are able to determine the preferred adsorption site for single molecules from calibrated STM data (Figure 10) by overlaying a copper substrate grid (see details in the Supporting Information). We found that single molecules are not adsorbed on the same site as molecules in structure A; the majority prefer the long-bridge adsorption site. We note, however, that for some molecules it is difficult to decide unambiguously whether the molecular centre is on a long-bridge or hollow site, perhaps due to the lower corrugation along this direction, which makes this the preferred diffusion direction of the molecule as it is for copper adatoms.[27]

To characterise the bonding behaviour and molecular conformation, we performed periodic DFT calculations of a single molecule adsorbed on a long-bridge site by using a sufficiently large unit cell to minimise intermolecular interactions (see the Supporting Information for details). A stable conformation of the molecule is found at this position, which undergoes considerable macrocycle distortions. Similarly to structure A, the cobalt atom in the core is situated very close to the substrate atoms, with a vertical distance of only 2.4 Å above the plane running through the top layer of copper atoms. The calculations result in a saddle-shaped molecular conformation, as shown in Figure 11a–c, and similar to that observed in other studies.[1a,2h,i,26] We find that the two pyrrole groups that are aligned with the [001] axis tilted upwards by 32° (Figure 11c) and the two [1$\bar{1}$0]-aligned pyrrole groups tilted downwards by 11–12° (Figure 11b), both with respect to the surface plane. Tilting of the phenyl groups is far less pronounced than for molecules accommodated in structure A, but greater phenyl twisting results in all four phenyl groups lying closer to the substrate plane. The calculated values for phenyl tilt and twist angles range between 167–170° and 29–30°, respectively; the latter can be compared with the calculated lowest energy conformation of Co-TPP in the gas phase, with resulting phenyl twist angles of 67 and 70°, and is, therefore, partly responsible for the saddling of the core as a consequence of steric repulsion from the phenyl rings.[2h] With lower phenyl twist angles, steric repulsion forces the macrocycle upwards or downwards, depending on whether the phenyls twist under or over the pyrrole groups (cf. Figure 11a), and the saddling is amplified by the small but notable upward tilts of the phenyl groups.

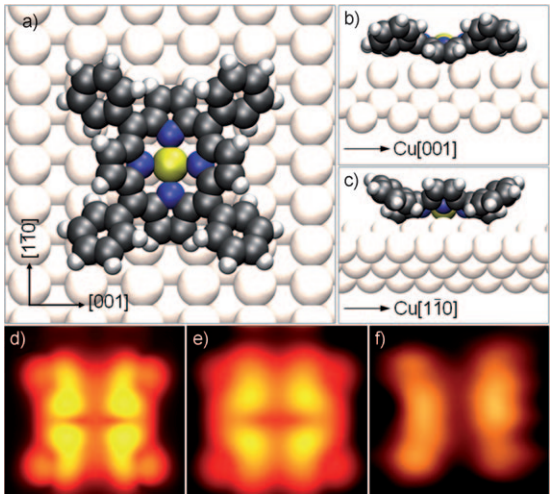

Figure 11. DFT calculation of the adsorption of a single Co-TPP molecule at the long-bridge site of Cu(110). a) The top-down view, showing the phenyl rings twisted partly below the pyrrole groups of the macrocycle, which induces a significant saddling of the core that becomes obvious when viewed along b) the Cu [1$\bar{1}$0] axis and c) the Cu [001] axis. Calculated STM images of the molecule at 1250 mV at tip-surface heights of 7 and 10 Å, respectively, are shown in d) and e). f) Experimental single molecule image at $V=1250$ mV, $I=0.4$ nA (19×20 Å^2). The copper axis in a) apply to d)–f).

We have performed DFT calculations of STM images for the stabilised single-molecule conformation (Figure 11d and e, with a tip–surface separation of 7 and 10 Å, respectively). For structure A, calculations with a tip height of 10 Å resulted in good agreement with experiment results (cf. Figure 5), but for the single-molecule comparison a slightly lower tip height might be justified. The calculated images resemble the major features of our experimental images (cf. Figure 11f); firstly, theoretical and experimental results both

show the single molecule with two symmetry lines aligned with the major copper axes. Secondly, we find agreement on a significant core contribution and experimentally resolve two elongated features either side of the centre, which reflect the four central spots in the calculated image (Figure 11d). Thirdly, the corner features related to the phenyl positions are broadened compared with structure A, which reflects the larger phenyl twist.

When deviating from the optimal gas-phase conformation, twisting the phenyl rings is more favourable than tilting.[2h] This is reflected in the reduced energy cost of 117 kJ mol^{-1} to deform a singly adsorbed molecule into the saddle conformation adsorbed at the long-bridge site, compared with 206 kJ mol^{-1} calculated for molecules in structure A in which the phenyls are strongly tilted. In addition, the cost of deforming the copper substrate is significantly lower for the singly adsorbed molecule, 19 kJ mol^{-1} rather than 31 kJ mol^{-1}. Thus, there is a significant reduction in E_{COST} from 237 kJ mol^{-1} for structure A molecules to 136 kJ mol^{-1} for the singly adsorbed molecules. We also calculated the gain in energy due to molecule–surface interactions for the single molecule on a long-bridge adsorption site, as we have done for structure A. In this case the value of $E_{MOL-SUR}$ was calculated to be -232 kJ mol^{-1}, which is again lower than the value of -335 kJ mol^{-1} calculated for structure A molecules. This finding is supported by the reduced electron transfer of 0.9 e$^-$ for the isolated molecule compared with 1.3 e$^-$ for a molecule in structure A. We found the bonding character to be very similar to that discussed for structure A, but weaker.

The energy balance results in an overall net gain of -96 kJ mol^{-1} for an isolated molecule adsorbed at the long-bridge position ($E^{LB}_{NET} = E_{MOL-SUR} + E_{COST}$), which is surprisingly close to the structure A value of -97 kJ mol^{-1} if inter-molecular interactions are ignored. A comparison of the energies involved shows that both the gain in energy due to the substrate interaction and the cost in energy due to deformation of the molecule and the copper substrate are significantly larger in magnitude for adsorbed Co-TPP within structure A than for a single molecule adsorbed in a long-bridge position. All energy contributions are summarised in Table 1. However, the net adsorption energy (ignoring inter-molecular interactions), changes very little, that is, the relative stability of the two conformations is almost equal. Therefore, the relatively small amount of energy (-58 kJ mol^{-1}) gained from the intermolecular π–π interactions between the tilted phenyl groups of the distorted molecules makes a crucial difference and is sufficient to promote the supramolecular assembly of structure A composed of Co-TPP molecules with a planar core and strong tilting deformations of the phenyl groups.

Conclusion

We have investigated the adsorption and organisation of Co-TPP at room temperature by using high-resolution STM experiments and periodic DFT calculations. The experimental data show self-organisation into two co-existing, highly ordered and stable mirror-image chiral domains that are formed from a single-molecule unit mesh that is commensurate with the surface. Periodic, semi-local DFT calculations were carried out for the experimentally observed unit mesh by, including both the molecular adlayer and a deformable copper surface, and π–π interactions were taken into account of by using the Langreth–Lundqvist van der Waals density functional.

Co-TPP molecules within the self-assembled structure adsorb at the short-bridge site of the Cu(110) surface. A considerable chemisorption interaction between the top layer of copper atoms and the entire Co-TPP macrocycle causes the molecule's core to be situated close to the substrate. This has two important effects: it maintains planarity of the core macrocycle and consequently induces significant tilt and twist deformations in two distinct pairs of diametrically opposite phenyls. The almost upright twisted phenyl groups in turn facilitate significant inter-molecular π–π interactions, contributing about -58 kJ mol^{-1} to the total domain energy. Within the 2D domains, the interplay between attractive inter-molecular interactions and steric repulsion forces each molecule to adopt a well-defined chiral propeller-like conformation, with clockwise propellers generating the A^{λ} domain, whereas the anticlockwise propellers generate the energetically equal but mirrored A^{δ} domain. Simulated STM images obtained from these structural models show very good agreement with the experimental data. The lack of porphyrin core structures in the STM images is primarily attributed to topographical effects due to strong phenyl tilting away from the surface and secondarily attributed to electron donation into the Co d_{z^2} orbital.

Furthermore, a comprehensive picture of the quantitative costs and gains of the relevant interactions that drive the substantial porphyrin deformation and the subsequent chiral organisation has been presented. Although the cost of the surface-induced deformations is very high at 237 kJ mol^{-1}, a favourable net interaction energy of about -156 kJ mol^{-1}

Table 1. Summary of costs, gains and molecular deformations for a single Co-TPP molecule within structure A and an isolated Co-TPP molecule.

Conformation	Φ [°]	Θ [°]	Height of Co above Cu [Å]	Shortest Co–Cu separation [Å]	$E_{MOL-SUR}$ [kJ mol^{-1}]	$E_{COST(MOL)}$ [kJ mol^{-1}]	$E_{COST(SUR)}$ [kJ mol^{-1}]	E_{GAIN} [kJ mol^{-1}]	E_{M-M} [kJ mol^{-1}]	E_{NET} [kJ mol^{-1}]
Molecule in structure A	154, 144, 152, 145	60, 88, 63, 79	2.2	2.5	−335	+206	+31	−97	−58	−156
Isolated molecule	167–170	29–30	2.4	–	−232	+117	+19	−96	–	−96

was calculated, with the strong molecule–substrate interaction of $E_{MOL-SUR} = -335\ kJ\,mol^{-1}$ more than compensating for the high costs of inducing molecular and substrate deformations.

In contrast, the singly adsorbed Co-TPP on Cu(110) is adsorbed at the long-bridge site and adopts the familiar saddle-shaped conformation. If inter-molecular interactions are ignored, we found the calculated adsorption energies of the saddle-shaped conformer and the highly distorted conformer to be almost equal. However, the phenyl tilting deformations of the latter generate favourable π–π interactions to give an additional interaction energy of $-58\ kJ\,mol^{-1}$ that drives supramolecular assembly and tips the system preference towards the distorted conformer.

In summary, our work highlights the need to adequately capture the full molecule–metal interaction to obtain an in-depth understanding of porphyrin behaviour at surfaces. In particular, we find strong molecule–metal interactions stabilising unexpected distortions in adsorbed porphyrin molecules. Additionally, such surface-induced deformations can be conducive for supramolecular assembly. Finally, this analysis of Co-TPP on Cu(110) may provide a more general framework for approaching the adsorption and assembly of large molecules on strongly interacting metal surfaces.

Experimental Section

Experimental details: LEED and STM experiments were performed under UHV conditions. STM images were acquired by using a Specs STM 150 Aarhus instrument. The STM was calibrated to >5% accuracy by measuring the specific distances of the O(2×1) superstructure following the introduction of oxygen onto the clean Cu(110) surface. All measurements were taken in constant current mode by using a tungsten tip and at a base pressure of 1.5×10^{-10} mbar. Bias voltages are measured at the sample ($V = V_{sample}$). STM images were enhanced by using WSxM[28a] and Image SxM.[28b]

The Cu(110) surface was a single crystal 8 mm in diameter and 1.8 mm thick (Surface Preparation Laboratory, NL), cut in the (110) plane to an accuracy of 0.5° and reported to be 99.999% pure and scratch free at ×800 magnification. The Cu(110) surface was prepared by using argon ion sputtering and annealing cycles, and atomic flatness and cleanliness were checked by STM and LEED prior to dosing the molecule. Co-TPP (Figure 1; Sigma–Aldrich) was used as purchased and sublimed at ≈430 K onto the Cu(110) surface, which was held at RT during deposition.

Computational details: The periodic DFT calculations in this study were performed by using version 4.6 of the VASP code.[29] Plane waves were used as a basis set with an energy cut-off of 400 eV. Valence electron–core interactions were included by using the projector-augmented wave method[30] and the generalised gradient approximation (PW91) was used for the exchange-correlation functional.[31] The π–π interactions between the phenyl groups of neighbouring molecules was accounted for by using an efficient implementation[18] of a post-correction scheme[19] of the Langreth–Lundqvist van der Waals density functional (vdW-DF).[19–20]

The calculations of Co-TPP in periodic structure A were based on a unit cell that was evaluated directly from LEED and STM data (see main text) and carried out on a 3×3×1 *k*-point grid. The copper surface was modelled by using a four-layer slab, with the bottom two layers fixed in their calculated bulk positions and the top two layers allowed to relax. The vacuum separation between the copper slabs was 16.8 Å, leaving about 10 Å between the molecule and the back of the next slab. Adsorption geometries were calculated by placing a Co-TPP molecule above the surface and allowing all molecular atoms and the top two layers of the copper slab to relax until all the forces on the atoms were less than $0.01\ eV\,Å^{-1}$. STM images were calculated using the Tersoff–Hamann approximation.[32]

The convergence with respect to calculational parameters was checked for the molecule–surface interaction. The energy deviated with less than $1.4\ kJ\,mol^{-1}$ if the *k*-point grid was increased to 6×6×1, the plane wave cut-off was increased from 400 to 500 eV or a full FFT grid was used to avoid wrap-around errors.

Calculations were also performed for a singly adsorbed Co-TPP molecule on Cu(110) by using a 6×8 surface unit cell that gave a minimum distance of 7.6 Å between the periodically repeated molecules and by using the same vacuum gap as in the periodic structure. In this larger supercell, a 2×2×1 *k*-point grid was sufficient to obtain converged results; all other parameters were the same. Following experimental evidence, the molecule was placed with the central cobalt atom above a long-bridge site on the surface and then a full geometry relaxation of the molecule and the top two layers was carried out.

To study the adsorption process, calculations were not only performed for the full adsorbate–surface system, but also on the isolated molecular overlayer and the isolated copper substrate in the same calculation supercell. Further calculations were performed on isolated Co-TPP molecules in vacuum. Calculations on isolated molecules were carried out in a larger $25\times25\times25\ Å^3$ supercell to minimise interactions with molecules in neighbouring cells. It was necessary to carry out spin-polarised calculations on the isolated monolayer and isolated molecules, but not on the adsorbed system because in this case the previously partially occupied Co d_{z^2} orbital becomes fully occupied. The known problem of semi-local DFT in the treatment of localised states, such as the 3d orbitals of Co,[33] may lead to some inaccuracy in the predicted amount of electron transfer between the substrate and the molecule, although we expect the direction and general extent of the electron transfer to be reproduced well. An improved treatment of the electron transfer may be possible by the inclusion of an on-site Coulomb term by using the GGA+U method or using more expensive calculations based introducing Hartree–Fock exchange, however, this is beyond the scope of the current calculations.

Acknowledgements

We are grateful to Dr S. Haq for obtaining the LEED data. A.R. and R.R. thank the EU Marie Curie Host Fellowship Program TANSAS (MTKD-CT-2005-029689) and the EU 7th Framework Small-Scale Collaborative Project RESOLVE (NMP4-SL-2008-214340) for support. P.D. is grateful to the UK Research Council EPSRC for a studentship. M.S.D. and M.P. would like to thank the Marie Curie Research Training Network PRAIRIES (contract MRTN-CT-2006-035810) and the Swedish Research Council (VR) for financial support. M.S.D. is grateful for funding of a post-doctoral fellowship and computational resources by the University of Liverpool.

[1] a) W. Auwärter, F. Klappenberger, A. Weber-Bargioni, A. Schiffrin, T. Strunskus, C. Woll, Y. Pennec, A. Riemann, J. V. Barth, *J. Am. Chem. Soc.* **2007**, *129*, 11279–11285; b) S. Yoshimoto, A. K. Tada, K. Suto, S. L. Yau, K. Itaya, *Langmuir* **2004**, *20*, 3159–3165; c) D. G. de Oteyza, I. Silanes, M. Ruiz-Oses, E. Barrena, B. P. Doyle, A. Arnau, H. Dosch, Y. Wakayama, J. E. Ortega, *Adv. Funct. Mater.* **2009**, *19*, 259–264.

[2] a) W. Auwärter, A. Weber-Bargioni, A. Riemann, A. Schiffrin, O. Groning, R. Fasel, J. V. Barth, *J. Chem. Phys.* **2006**, *124*, ; b) J. M. Gottfried, K. Flechtner, A. Kretschmann, T. Lukasczyk, H. P. Steinruck, *J. Am. Chem. Soc.* **2006**, *128*, 5644–5645; c) C. Humbert, C. Volcke, Y. Sartenaer, A. Peremans, P. A. Thiry, L. Dreesen, *Surf. Sci.* **2006**, *600*, 3702–3709; d) A. Ogunrinde, K. W. Hipps, L. Scudiero, *Langmuir* **2006**, *22*, 5697–5701; e) F. Buchner, K. Comanici,

N. Jux, H. P. Steinrueck, H. Marbach, *J. Phys. Chem. C* **2007**, *111*, 13531–13538; f) T. Lukasczyk, K. Flechtner, L. R. Merte, N. Jux, F. Maier, J. M. Gottfried, H. P. Steinruck, *J. Phys. Chem. C* **2007**, *111*, 3090–3098; g) A. Weber-Bargioni, W. Auwärter, F. Klappenberger, J. Reichert, S. Lefrancois, T. Strunskus, C. Woll, A. Schiffrin, Y. Pennec, J. V. Barth, *ChemPhysChem* **2008**, *9*, 89–94; h) T. Wölfle, A. Görling, W. Hieringer, *Phys. Chem. Chem. Phys.* **2008**, *10*, 5739–5742; i) J. M. Gottfried, H. Marbach, *Z. Phys. Chem. (Muenchen, Ger.)* **2009**, *223*, 53–74.

[3] a) R. Hausschild, G. Reidel, J. Zeller, H. Kalt, *VDI Berichte* **2004**, 119–122; b) K. P. Jensen, U. Ryde, *ChemBioChem* **2003**, *4*, 413–424.

[4] N. A. Rakow, K. S. Suslick, *Nature* **2000**, *406*, 710–713.

[5] a) F. Moresco, G. Meyer, K. H. Rieder, H. Tang, A. Gourdon, C. Joachim, *Phys. Rev. Lett.* **2001**, *86*, 672–675; b) F. Moresco, G. Meyer, H. Tang, C. Joachim, K. H. Rieder, *J. Electron Spectrosc. Relat. Phenom.* **2003**, *129*, 149–155.

[6] C. Li, J. Ly, B. Lei, W. Fan, D. H. Zhang, J. Han, M. Meyyappan, M. Thompson, C. W. Zhou, *J. Phys. Chem. B* **2004**, *108*, 9646–9649.

[7] Y. He, T. Ye, E. Borguet, *J. Am. Chem. Soc.* **2002**, *124*, 11964–11970.

[8] a) T. Kamikado, T. Sekiguchi, S. Yokoyama, Y. Wakayama, S. Mashiko, *Thin Solid Films* **2006**, *499*, 329–332; b) F. Nishiyama, T. Yokoyama, T. Kamikado, S. Yokoyama, S. Mashiko, *Appl. Phys. Lett.* **2006**, *88*, ; c) T. Sekiguchi, Y. Wakayama, S. Yokoyama, T. Kamikado, S. Mashiko, *Thin Solid Films* **2004**, *464–465*, 393–397; d) T. Yokoyama, S. Yokoyama, T. Kamikado, S. Mashiko, *J. Chem. Phys.* **2001**, *115*, 3814–3818; e) T. Yokoyama, S. Yokoyama, T. Kamikado, Y. Okuno, S. Mashiko, *Nature* **2001**, *413*, 619–621; f) T. A. Jung, R. R. Schlittler, J. K. Gimzewski, *Nature* **1997**, *386*, 696–698; g) W. Auwarter, K. Seufert, F. Klappenberger, J. Reichert, A. Weber-Bargioni, A. Verdini, D. Cvetko, M. Dell′Angela, L. Floreano, A. Cossaro, G. Bavdek, A. Morgante, A. P. Seitsonen, J. V. Barth, *Phys. Rev. B* **2010**, *81*; h) J. Brede, M. Linares, S. Kuck, J. Schwobel, A. Scarfato, S.-H. Chang, G. Hoffmann, R. Wiesendanger, R. Lensen, P. H. J. Kouwer, J. Hoogboom, A. E. Rowan, M. Broring, M. Funk, S. Stafstrom, F. Zerbetto, R. Lazzaroni, *Nanotechnology* **2009**, *20*, 275602.

[9] a) K. W. Hipps, X. Lu, X. D. Wang, U. Mazur, *J. Phys. Chem.* **1996**, *100*, 11207–11210; b) X. Lu, K. W. Hipps, X. D. Wang, U. Mazur, *J. Am. Chem. Soc.* **1996**, *118*, 7197–7202.

[10] M. Gruden-Pavlovic, S. Grubisic, S. R. Niketic, *J. Inorg. Biochem.* **2004**, *98*, 1293–1302.

[11] I. Mochida, K. Suetsugu, H. Fujitsu, K. Takeshita, K. Tsuji, Y. Sagara, A. Ohyoshi, *J. Catal.* **1982**, *77*, 519–526.

[12] D. Ecija, M. Trelka, C. Urban, P. de Mendoza, E. Mateo-Marti, C. Rogero, J. A. Martin-Gago, A. M. Echavarren, R. Otero, J. M. Gallego, R. Mirandat, *J. Phys. Chem. C* **2008**, *112*, 8988–8994.

[13] T. E. Shubina, H. Marbach, K. Flechtner, A. Kretschmann, N. Jux, F. Buchner, H. P. Steinruck, T. Clark, J. M. Gottfried, *J. Am. Chem. Soc.* **2007**, *129*, 9476–9483.

[14] C. Mück-Lichtenfeld, S. Grimme, *Mol. Phys.* **2007**, *105*, 2793–2798.

[15] D. G. de Oteyza, I. Silanes, M. Ruiz-Oses, E. Barrena, B. P. Doyle, A. Arnau, H. Dosch, Y. Wakayama, J. E. Ortega, *Adv. Funct. Mater.* **2009**, *19*, 259–264.

[16] L. A. Zotti, G. Teobaldi, W. A. Hofer, W. Auwarter, A. Weber-Bargioni, J. V. Barth, *Surf. Sci.* **2007**, *601*, 2409–2414.

[17] K. Leung, S. B. Rempe, P. A. Schultz, E. M. Sproviero, V. S. Batista, M. E. Chandross, C. J. Medforth, *J. Am. Chem. Soc.* **2006**, *128*, 3659–3668.

[18] A. Gulans, M. J. Puska, R. M. Nieminen, *Phys. Rev. B* **2009**, *79*.

[19] M. Dion, H. Rydberg, E. Schroder, D. C. Langreth, B. I. Lundqvist, *Phys. Rev. Lett.* **2004**, *92*.

[20] a) M. Dion, H. Rydberg, E. Schroder, D. C. Langreth, B. I. Lundqvist, *Phys. Rev. Lett.* **2005**, *95*; b) T. Thonhauser, V. R. Cooper, S. Li, A. Puzder, P. Hyldgaard, D. C. Langreth, *Phys. Rev. B* **2007**, *76*.

[21] S. M. Barlow, R. Raval, *Surf. Sci. Rep.* **2003**, *50*, 201–341.

[22] K. Hermann, M. A. Van Hove, LEEDpat - a LEED pattern simulator, September **2002**.

[23] W. Tang, E. Sanville, G. Henkelman, *J. Phys. Condens. Matter* **2009**, *21*, 084204.

[24] a) A. Puzder, M. Dion, D. C. Langreth, *J. Chem. Phys.* **2006**, *124*; b) T. Thonhauser, A. Puzder, D. C. Langreth, *J. Chem. Phys.* **2006**, *124*.

[25] a) M. O. Sinnokrot, C. D. Sherrill, *J. Phys. Chem. A* **2006**, *110*, 10656–10668; b) S. Grimme, C. Muck-Lichtenfeld, J. Antony, *Phys. Chem. Chem. Phys.* **2008**, *10*, 3327–3334; c) S. Tsuzuki, K. Honda, T. Uchimaru, M. Mikami, K. Tanabe, *J. Am. Chem. Soc.* **2002**, *124*, 104–112.

[26] a) W. Auwärter, A. Weber-Bargioni, S. Brink, A. Riemann, A. Schiffrin, M. Ruben, J. V. Barth, *ChemPhysChem* **2007**, *8*, 250–254; b) M. Eichberger, M. Marschall, J. Reichert, A. Weber-Bargioni, W. Auwarter, R. L. C. Wang, H. J. Kreuzer, Y. Pennec, A. Schiffrin, J. V. Barth, *Nano Lett.* **2008**, *8*, 4608–4613.

[27] H. Yildirim, A. Kara, S. Durukanoglu, T. S. Rahman, *Surfactant Sci. Ser.* **2006**, *600*, 484–492.

[28] a) I. Horcas, R. Fernandez, J. M. Gomez-Rodriguez, J. Colchero, J. Gomez-Herrero, A. M. Baro, *Rev. Sci. Instrum.* **2007**, *78*, 013705; b) S. D. Barrett, Image SXM, **2010**, http://www.ImagesSXM.org.uk.

[29] G. Kresse, J. Furthmüller, *Phys. Rev. B* **1996**, *54*, 11169–11186.

[30] G. Kresse, D. Joubert, *Phys. Rev. B* **1999**, *59*, 1758–1775.

[31] J. P. Perdew, J. A. Chevary, S. H. Vosko, K. A. Jackson, M. R. Pederson, D. J. Singh, C. Fiolhais, *Phys. Rev. B* **1992**, *46*, 6671–6687.

[32] J. Tersoff, D. R. Hamann, *Phys. Rev. Lett.* **1983**, *50*, 1998–2001.

[33] C. J. Cramer, D. G. Truhlar, *Phys. Chem. Chem. Phys.* **2009**, *11*, 10757–10816.

Received: June 23, 2010
Published online: September 17, 2010

